Roughness and scaling in cellular patterns: analysis of a simple model

2001 J. Phys. A: Math. Gen. 34 6225

(http://iopscience.iop.org/0305-4470/34/32/302)

INSTITUTE OF PHYSICS PUBLISHING JOURNAL OF PHYSICS A: MATHEMATICAL AND GENERAL

J. Phys. A: Math. Gen. **34** (2001) 6225–6238 PII: S0305-4470(01)21375-4

Roughness and scaling in cellular patterns: analysis of a simple model

C Oguey[1] **and N Rivier**[2]

[1] LPTM, Université de Cergy-Pontoise, 95031 Cergy-Pontoise, France
[2] LDFC, ULP, 67084 Strasbourg, France

E-mail: oguey@ptm.u-cergy.fr and nick@ldfc.u-strasbg.fr

Received 22 January 2001, in final form 11 June 2001
Published 3 August 2001
Online at stacks.iop.org/JPhysA/34/6225

Abstract

A foam can be decomposed into successive layers of cells at the same topological distance to an origin, which is either an arbitrary cell or a basal plane. The shape of these layers (profile and thickening) indicates the degree of randomness of the cellular pattern. To support this idea, we analyse the layer shapes in 2D rectangular models of foam. As confirmed by numerical simulations, the fluctuations in the direction normal to the layers are self-affine on a significant range of scales, with values of the exponents compatible with the KPZ universality class: $\zeta \simeq 0.5$ for the roughness exponent and $z \simeq 1.5$ for the dynamic exponent measuring the increase of the intralayer correlation length ξ. These fluctuations are not sufficient, however, to affect the dominant behaviour of the number of cells per layer, found to saturate in cylindrical geometry, and to increase linearly in concentric geometry.

PACS numbers: 47.53.+n, 83.80.Iz

1. Introduction

In the coarsening process of foams, large bubbles grow at the expense of smaller ones which shrink and eventually disappear. From this basic feature, one may expect large discrepancies in the size of bubbles. This, together with the fact that small units put together may build larger ones, makes it plausible that foams obey some self-similar or fractal types of arrangement, at least in suitable regimes like the late stage scaling state where the foam remains stationary overall; only the mean bubble size increases with time.

Conjectures of this type were made earlier [1–3]. Even if, nowadays, fractal models of foams are regarded as unrealistic, fractal geometry may still describe some partial, specific aspects of those irregular structures. This is the aim of the present paper.

Our concern will be the fluctuations and populations of the layers into which any cellular pattern can be decomposed. Through the study of simplified, but significant models, we

will show that, because of a competition between disorder and artificial nearest-neighbour correlations built in the geometrical definition of layers, the fluctuations of the layers adopt self-affine profiles similar to those characteristic of aggregation–deposition phenomena in solid state growth.

Foams are regular, yet topologically disordered patterns. Regularity is exhibited locally—every vertex has minimal valencies (number of incident edges, interfaces, cells, etc) [4], so that the edges of a two-dimensional foam form a regular graph of valency 3—but also globally: the foam is uniform overall. This overall uniformity is a thermodynamic steady state, characterized by maximum entropy, a few observable equations of state (known as Aboav–Weaire, Lewis, etc, laws) and Boltzmann-like distributions of cells (the probability that a cell has $n = 3, 4, \ldots$ neighbours) [5].

An effect of disorder is that the outer contour of layer j wiggles substantially. But this roughening is limited by the correlations imposed by space-filling. The simple model studied in this paper has been introduced to understand this effect. The definition of successive layers at increasing distances j from the origin implies that the *static* roughening in foams and the non-equilibrium roughening of a growing interface in crystal growth or in aggregation are closely related problems.

2. Layers

2.1. Topological distance

The constraints of space-filling by topological polygons impose observable correlations between cells [5]. In foams or similar assemblies of cells with fairly uniform sizes, because of randomness, it is often more appropriate to account for correlations in terms of topology than metrics. The topological distance between cells is defined as the minimum number of boundaries (films in real foams) one has to cross (transversally) to join the interior of two cells. Alternatively, this is the natural topological distance in the dual graph, where each cell is a point and each dual bond counts for one along a minimizing path. Thus any cell is at distance 0 from itself. Nearest neighbours, sharing a common facet, are at distance 1 from each other.

Around any particular cell, taken as the origin $j = 0$, the cells can be classified into *layers*, labelled by $j = 1, 2, 3, \ldots$, the set of all cells at distance j from the origin [4, 6–11][3]. Thus, layers are equivalent to coordination shells in the dual graph[4] [10, 12–14].

All the cells in layer j are nearest neighbours to at least one cell in layer $j - 1$. Many, but not all, cells are also neighbours to cells in layer $j + 1$. The cells which have no contact with any one in layer $j + 1$ are called defect inclusions (or singular cells) [6]. Members of isolated clusters are also considered as defects. A *shell* is the closed contour of interfaces (edges in 2D) forming the outer boundary of a layer. In 2D, a shell j consists of edges separating j and $(j + 1)$ cells. By convention, it is a topological circle. More precise definitions are given in the appendix.

Here, we shall also measure distance from a (flat) ground ($y = 0$). In this case, a layer is the set of cells at distance j from the ground (with periodic boundary conditions in the horizontal direction, the overall geometry becomes cylindrical).

[3] An n corona, as used in [11], is equivalent to the union of layers $j = 0, \ldots, n$.

[4] In general, the dual is a multi-graph, with more than one bond connecting two nodes. Only with suitable restrictions does it become a graph. This is discussed in [8] in another terminology. Here, we will always assume that the dual of a foam is a graph—excluding cells with 1 or 2 edges, double contacts, etc. Two neighbouring cells, separated by an interface (common side in 2D), are represented, in the dual graph, by two vertices linked by an edge (in any dimensions).

2.2. Correlations and populations

Given the decomposition of a foam into layers, what is the number of cells K_j in each layer $j = 1, 2, 3, \ldots$? What is its typical—or average—behaviour for large j? In this section, these statements are given for concentric geometry.

Comparing some of their formulae with data from quasi-2D soap froths and from Voronoi models, Aste *et al* [15] observe that 'experimentally, the number of cells per layer increases linearly in j after the first few layers'. Similar conclusions were drawn from numerical simulations in [8, 9]. With more speculation, the subject is also treated in [16]. K_j linear in j is often called the *Euclidean* hypothesis.

If the size distribution is well behaved (with bounded moments) and if the layers are ordered increasingly, $\langle K_j \rangle$ is proportional to the geometrical measure M_j of the j shell: length in 2D foams, area in 3D ones.

A priori, if the shells behave like smooth closed surfaces at large scale, we expect M_j to be of the order of j^{D-1}. If, on the other hand, the shells are wildly shaken by randomness (like random walks in 2D), then $M_j \sim j^{\nu}$, with an exponent larger than $D-1$ but presumably smaller than D because of self-avoidance. The layers are then rougher.

A power law behaviour $M_j \sim j^{\nu}$ means that the foam is self-affine, a type of fractal symmetry [17–19]. If such a power law holds, then the value of the exponent is a quantitative signature of the degree of disorder. Lower values (closer to $D-1$) correspond to weakly random patterns (extreme cell sizes less likely, smooth shell shapes at large distances), higher values ($D-1 < \nu < D$) characterize more disordered foams (large deviations in sizes, shells behaving like random walks or surfaces, large proportion of inclusions).

The present paper is mainly devoted to investigating these geometrical features in a simplified—but tractable—model. As shown in [8], correlations are closely related to concentric populations around cells: for example, expressing the pair correlation $A_j(k, n)$ (k- and n-sided cells at mutual distance j) as a function of j and of the topological charges $(6-k)$ and $(6-n)$ involves the same coefficients as for K_j.

3. A Cartesian model: tower foams

The model retains some essential features of real foams: randomness, space filling, coordination 3. It also has artefacts, which make it accessible to theory but have a more tenuous correspondence with reality: there are no triangular cells, the cell sizes are integer numbers, with a minimal area of two, and the disorder is confined to only one direction in space.

Analysis of artificial models is classic in foams [20]. Even if this would require further investigations and proofs, we believe that, since our questions are chiefly topological in nature, our minimal model retains enough characteristics of foams to make our conclusions valid for a broader category of cellular patterns, including real foams.

Before defining the model, let us give an argument showing that the absence of triangles is not relevant.

3.1. The role of triangles in 2D foams

In the partition into layers, triangular cells are always defect inclusions. Moreover, extinction (the so-called $T2$ elementary topological transformation) of an isolated triangle does not change the layer structure, in the sense that any cell belonging to layer j ($j = 0, 1, 2, \ldots$) before extinction still belongs to layer j after extinction (whereas this may no longer be the case under

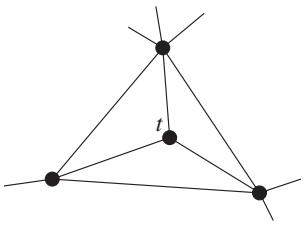

Figure 1. Dual graph of a triangle t and its three neighbours.

extinction of an n-sided cell, $n \geqslant 4$). This property holds for any choice of decomposition into layers, that is, whichever (non-triangular) cell or plane is chosen as origin.

To prove this fact, consider the pattern dual to a triangular cell (figure 1). To join two cells (vertices in the dual graph, excluding the triangle t itself), it is always shorter to take one of the external edges than to go through the central three-fold star t. Therefore, no minimizing path goes through t and deleting t will not change any numbering.

The same property holds if there are more than one vertex inside a dual triangle. In fact, any finite pattern compatible with the general prescriptions of the foam (e.g. generic coordination 3 in the direct graph) is acceptable inside the outer triangle as long as the boundary (the outer triangle itself) is not changed. In the direct graph, this corresponds to a finite patch that is connected to the rest of the graph by only three bonds: a 'tripod'. Tripods are always defects, regardless of the origin (as long as it is outside the tripod).

As a consequence, the layer structure is affected by the presence of triangles only in a reducible way. Creating or destroying triangles does not change the distance of any other cell to the origin (thus to which layer a cell belongs). So, if the layer sequence is appropriate to characterize the type of given cellular patterns, we should seek 'robust' numbers, independent of the triangles. For example, the population K_j does not meet this criterion. Neither does the topological charge Q_j of layer j. But the number of regular cells does: $K_j^{\mathrm{r}} = K_j - K_j^{\mathrm{def}}$. The charge enclosed by the j shell, $\sum_{i=0}^{j} Q_i$, would, if there was no triangle edge on the boundary (= shell).

3.2. Definition

The model is a 2D packing of columnar cells, each of unit width (in the horizontal, x, direction) and of random length s (height in the vertical, y, direction). The sizes (s is both length and area) of the individual cells are taken as independent random variables, identically distributed with exponential law:

$$\Pr(s) = \frac{1-q}{q}\, q^{s/2} \qquad s = 2, 4, 6, \ldots . \tag{1}$$

The parameter q has a fixed value in $]0, 1[$. It controls the mean cell size through $\langle s \rangle = 2/(1-q)$, which tends to infinity as $q \to 1$. Unless otherwise stated, we will take $q = 1/2$, $\langle s \rangle = 4$.

The foam lies on a semi-infinite vertical cylinder, a domain of width L with periodic boundary conditions in the x direction. The bottom has a crenellated profile: $y_0 = x \bmod 2$. This profile and even values for the cell lengths ensure that vertices have coordination 3, as in real foams. The system is unbounded in the positive y direction.

Some epithelial tissues have a columnar geometry similar to the present model [21].

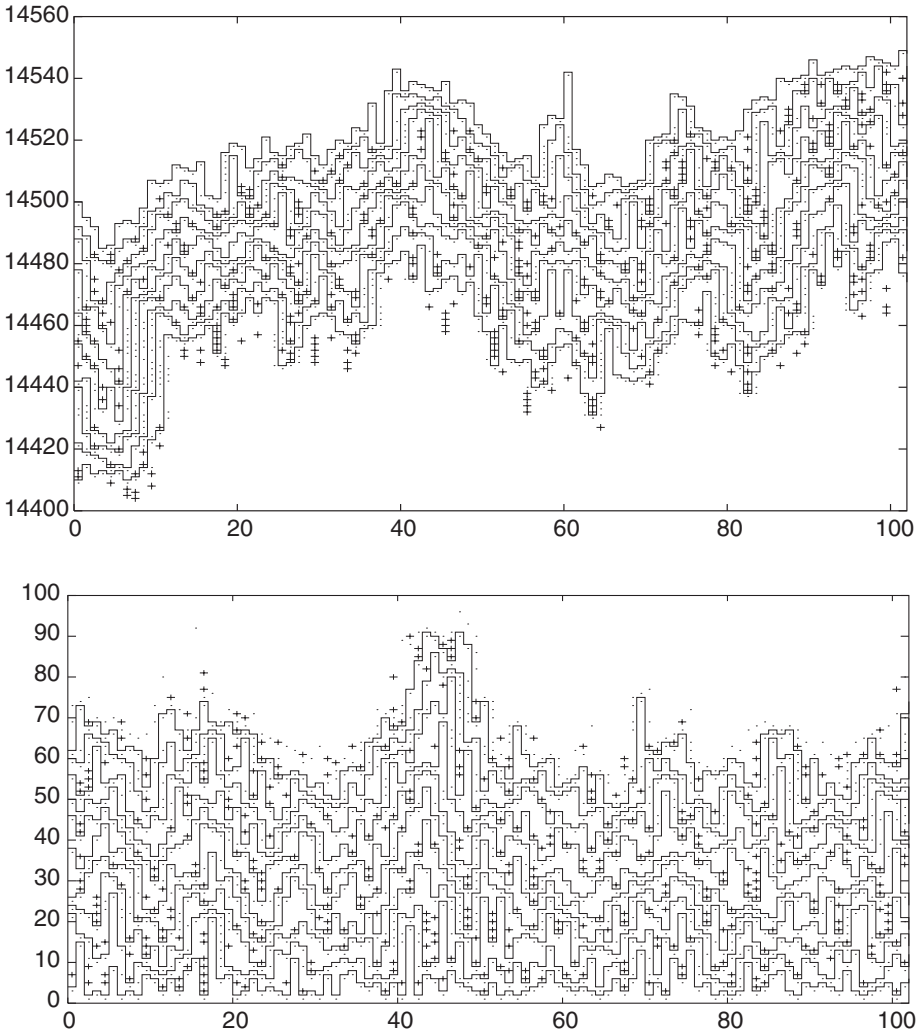

Figure 2. First columns of the bottom layers, $j \leqslant 10$, (bottom) and of the layers in the range $j \sim 2000$ (top) of a typical simulation ($L = 1000$). To avoid overloading the picture, the cell boundaries are not drawn (except for the part belonging to layer boundaries). Instead, the following convention is used: the top square of each cell (each cell is a pile of squares) is marked by a dot ($\cdot$) when the cell is regular and by a cross (+) when it is a defect (= inclusion) [4, 9].

3.3. Simulations

Simulations are carried out on systems of over 2×10^6 cells, that is $L = 1000$ and $j = 0, \ldots, 2000, \ldots$. The jth shell is described by a profile function $h_j : y = h_j(x)$, periodic in x with period L. The aspect of the foam and some of its layers are shown in figure 2.

The mean vertical position of shell j, $\overline{h_j} = L^{-1} \int_0^L h_j(x)\,\mathrm{d}x$ is linear in j, up to small fluctuations. The mean rise (average slope) is the product of the mean cell size by the mean number v of cells per column in each layer. According to figure 3 (top), the average vertical thickness is $v = 1.81\ldots$ cells in the stationary regime.

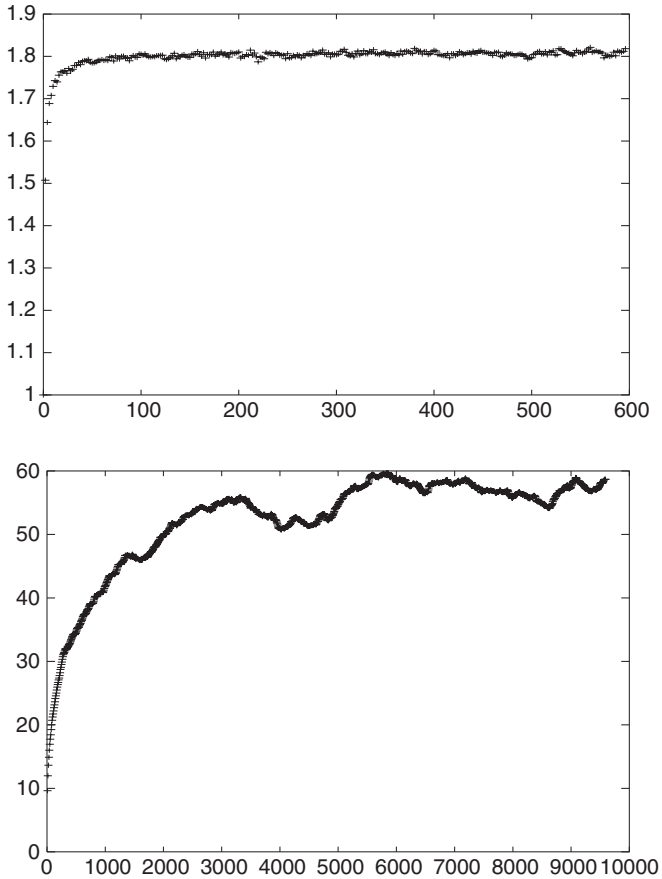

Figure 3. Top: the number of cells per layer divided by L versus j. This quantity is the velocity v at which the front moves vertically (in units of cells, considering j as time). Bottom: the fluctuations $\sigma(h_j)$ as a function of j. In both graphs, an average has been taken over 50 samples.

3.4. Profile fluctuations

The striking feature is that the deviation (rms) of h_j:

$$\sigma(h_j) = \left\langle \left(\frac{1}{L} \int_0^L \left(h_j(x) - \overline{h_j} \right)^2 \, \mathrm{d}x \right)^{1/2} \right\rangle \tag{2}$$

is bounded; it saturates at large j (figure 3 (bottom)). $\langle \cdots \rangle$ stands for the average over samples or disorder. If, instead of the topological distance, we had measured the Euclidean height of the jth cell in each column, we would have found a rms growing like $j^{1/2}$ (law of large numbers). The constant asymptotic behaviour indicates a transverse rigidity (correlation) in the layers. Note that this rigidity is not a consequence of the statistics of the cells, independent by construction. The correlation is geometrical, entirely contained in the way the layers are defined.

As the cells are identically distributed in size throughout the whole foam (in particular their mean size $\langle s \rangle$ is constant), the number of cells is related to the shape of the layer profile; to a first approximation, K_j is proportional to the length of the graph of h_j (curve $h_j(x)$ in 2D). The fact that the fluctuations are bounded implies that K_j is also bounded (section 3.6).

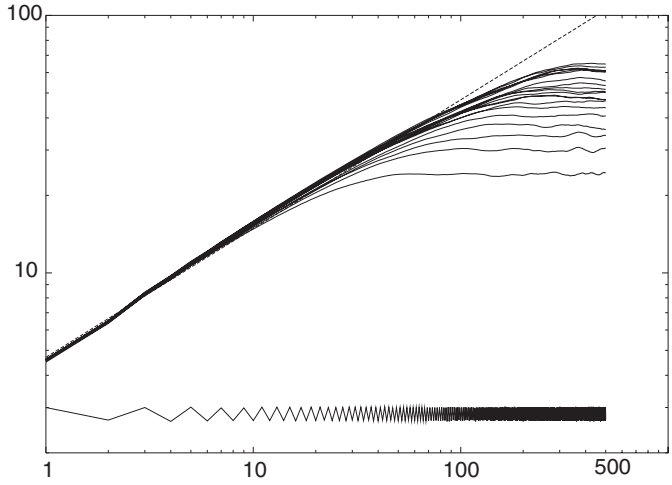

Figure 4. Equal time correlation g_j versus horizontal distance x, sampled for values of j ranging from 1 (lower curve) to $j_{\max} \simeq L^{3/2}$ (log–log plot). The curves $g_j(x)$ are periodic in x with period L and symmetric about $x = 0$ and $L/2$. The broken line has slope 0.5.

3.5. Profile correlations

These characteristics are corroborated by analysing the profile correlation function

$$g_j(x) = \langle \overline{|h_j(k+x) - h_j(k)|} \rangle \tag{3}$$

(average taken over $k = 1, \ldots, L$ and over samples). The following properties are directly observed in simulations (figure 4). As the layer number j increases, the correlation function converges to a stationary profile, ultimately independent of j. The convergence is fast at small distance $|x|$ and takes progressively longer to settle at larger distances. The slope of the log plot (figure 4) gives the wandering, or roughness, exponent ζ [22, 23]. The value found here is $\zeta = 0.50 \pm 0.01$.

The finite size of the system has no significant effect over a range of $|x|$ small compared to $L/2$. However, the saturation value (g reaches a maximum near $x = L/2$) depends on sample size L. The dependence on L is discussed further in section 4.

3.6. Layer size

The size (here length) M_j of shell j is the sum of its horizontal component L (or L_j if it depends on j, as in section 5.1) and of the vertical steps: $\sum_{x=0}^{L-1} |h_j(x+1) - h_j(x)|$; on average, the latter is proportional to the correlation function (3), so that

$$\langle M_j \rangle = \big(1 + g_j(1)\big)\, L_j. \tag{4}$$

There is a similar expression for the population $\langle K_j \rangle$; indeed, since proper inclusion clusters do not occur in columnar models, $\langle K_{j+1} \rangle$ is proportional to $\langle M_j \rangle$ by a dimensional factor related to cell size $\langle s \rangle$.

Thus, the relatively fast convergence of the layer size to its asymptotic behaviour (a constant value in cylindrical geometry, linear in j in concentric geometry, see section 5.1) is due to the rapid convergence of the pair correlation at short range ($x = 1$). The fact that $\langle M_j \rangle$ does not depend on longer range correlations, linked to slower processes, certainly contributes

to its stability. But the drawback is that this quantity tells us little, eventually, on the nature of (dis)order in the system.

4. Connection with aggregation models—scaling

As already suggested by the title and figures, there is a close relation between our layer profiles and the non-equilibrium problems of crystal growth, aggregation, ballistic deposition, etc (see [17–19] for reviews). Our layers have nothing to do with crystal planes. They are related to the shape of the crystal surface as it evolves over time (by aggregation, deposition, contamination, etc). The correspondence is

foams:	j	successive layers
aggregates:	t	evolving surface

By definition layer $j+1$ entirely covers layer j. In the Manhattan geometry of our model, this means that the $(j+1)$ cells must cover not only the j cells on top (local maxima, plateaux or minima where the defects sometimes occur) but also the vertical sides (cliffs) of shell j. Hence the height function h_j satisfies conditions of the type

$$h_{j+1}(x) \geqslant \max(h_j(x-1), h_j(x), h_j(x+1)), \qquad \forall x. \tag{5}$$

Such rules are at the basis of a number of models of deposition–aggregation. How the profile shape is influenced by the precise settings of the rules (equation of motion) was analysed in [24].

Most of the results we use here are from scaling theory, which is known to be valid in such phenomena. Scaling theory is based on the assumption that the profile is self-affine; define δh_j as the difference between the local and average heights:

$$\delta h_j(x) = h_j(x) - L^{-1} \int_0^L h_j(x')\,\mathrm{d}x'. \tag{6}$$

A self-affine behaviour means that there are exponents z, ζ such that, for all λ (compatible with physical length scales), $\lambda^{\zeta}\delta h_{\lambda^z j}(\lambda x)$ has the same statistical properties as $\delta h_j(x)$ [19, 22, 23]. That is, if x scales with λ, the time j scales as λ^z, and the profile δh as λ^{ζ} where z and ζ are, respectively, the dynamical and the roughness exponents.

The values of the exponents can be deduced from the fluctuations $\sigma(h_j)$ as well as from the correlation function g_j, both depending on j and L. In the model, these two functions have, indeed, a behaviour typical of scaling.

In section 3.5 on the correlations (in particular figure 4), we already found that the exponents were $\zeta \simeq 0.5$ and $z \simeq 3/2$ (from $j_{\max} \simeq L^z$).

At small values of j, the mean fluctuations of the layer profile are not sensitive to system size L (provided, only, that $L > j$) (figure 5 (top)). They fit a power law with exponent $\beta = 0.34 \pm 0.02$.

At large j (or time), the fluctuations saturate (figure 3 (bottom)) to a stationary value $\sigma(h_\infty)$ depending on L (figure 5 (bottom)). Least square fit yields, again, the roughness exponent $\zeta = 0.51 \pm 0.01$.

The ratio of these values is the dynamical exponent [22, 23, 25] giving the spread in time of the correlation length: $\xi_j \sim j^{1/z}$. Here, we get $z = \zeta/\beta \simeq 1.5$. These values agree with those found in section 3.5.

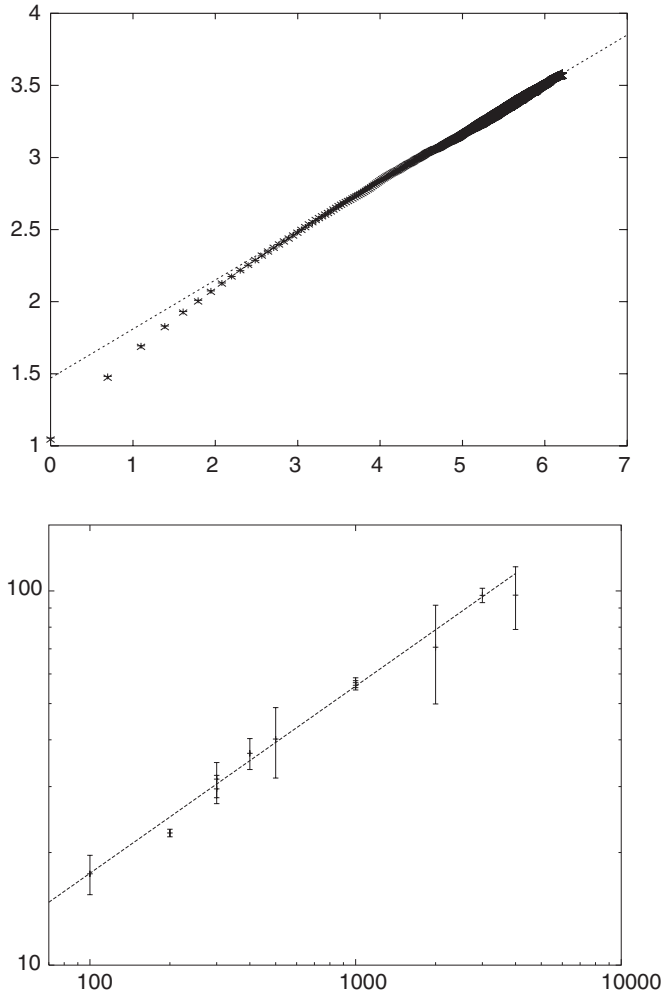

Figure 5. Top: log–log plots of the mean fluctuations of the layer profile, $\sigma(h_j)$, versus j for small values of j. The points are for $L = 1600$ ($\times$) and $L = 6400$ (+); the broken line (fit) has slope 0.34. Bottom: the saturation value $\sigma(h_\infty)$ as a function of L. Slope of the fit: 0.508.

5. Variants

5.1. Conical boundary conditions

To get a closer estimate of the populations of concentric layers around a central cell, we have changed the boundary conditions from cylindrical to conical. Instead of being constant, the imposed horizontal period now depends on j as $L_j = 100{+}2j$. At each step, layer $j{+}1$ is built over layer j as before, but now stacking cells independently into $L_{j+1} = L_j + 2$ columns. Similarly, the cells in layer $j + 2$ will be chosen independently over $L_{j+2} = L_j + 4$ columns, and so on.

The resulting cell population, shown in figure 6, converges towards an affine function of j. Measured in cells per column, the slope quickly converges to the constant $v = 1.808\ldots$, which is, within error bars, the same as in section 3.3. Indeed, the nearest-neighbour correlation is practically insensitive to the boundary conditions.

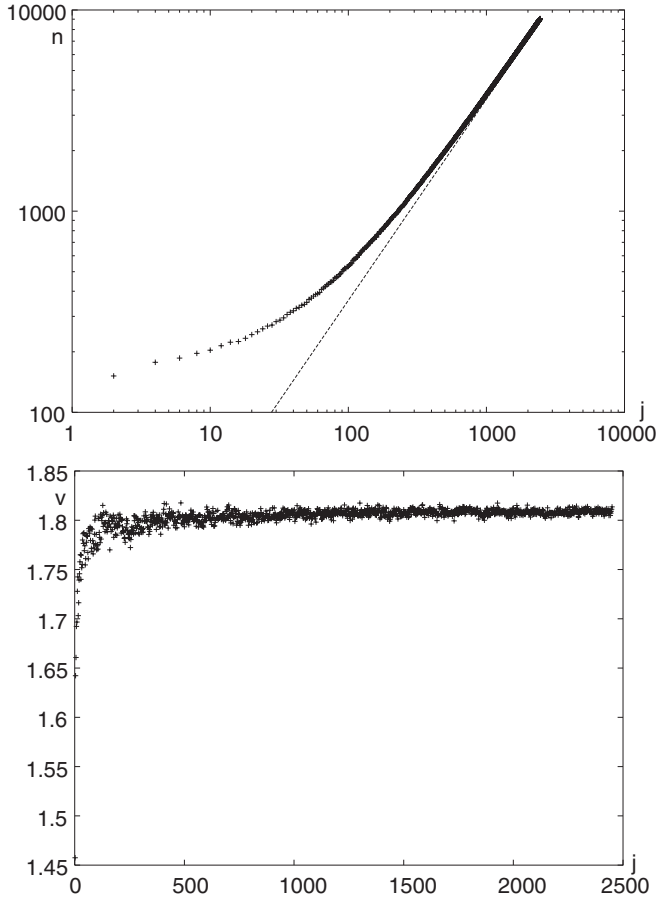

Figure 6. Layer population in conical geometry, averaged over 50 samples. Top: the number of cells K_j per layer as a function of j (log–log). Bottom: the 'velocity' v_j $(= K_j/L_j)$ versus j.

5.2. Inhomogeneous cell distributions

To confirm the transversal rigidity of the layers, we have also tested an inhomogeneous model: the cell size distribution is no longer constant but it varies from column to column. In (1), the parameter q now depends on x as

$$q(x) = \frac{3}{4} - \left| \frac{x}{2L} - \frac{1}{4} \right| \qquad 0 \leqslant x \leqslant L \tag{7}$$

('gradient model'). So the average cell size $\langle s \rangle(x)$ varies from 4 (near the edges of the box) to 8 (in the middle). Since the velocity is proportional to $\langle s \rangle$, we might have thought that, in the absence of correlations, the centre would grow twice as fast as the flanks, so that the average slope of the profile would *increase* with altitude (j). But, as figure 7 (top) shows, this is not the case: after the first layers (transient regime, not shown), the slope of the profile quickly *saturates* to a steady value. This is another effect of the correlation induced by the layer representation.

Another manifestation of this saturation is that the mean layer thickness quickly reaches a steady regime fluctuating around the average value of $v = 2.93\ldots$ cells (figure 7 (bottom)).

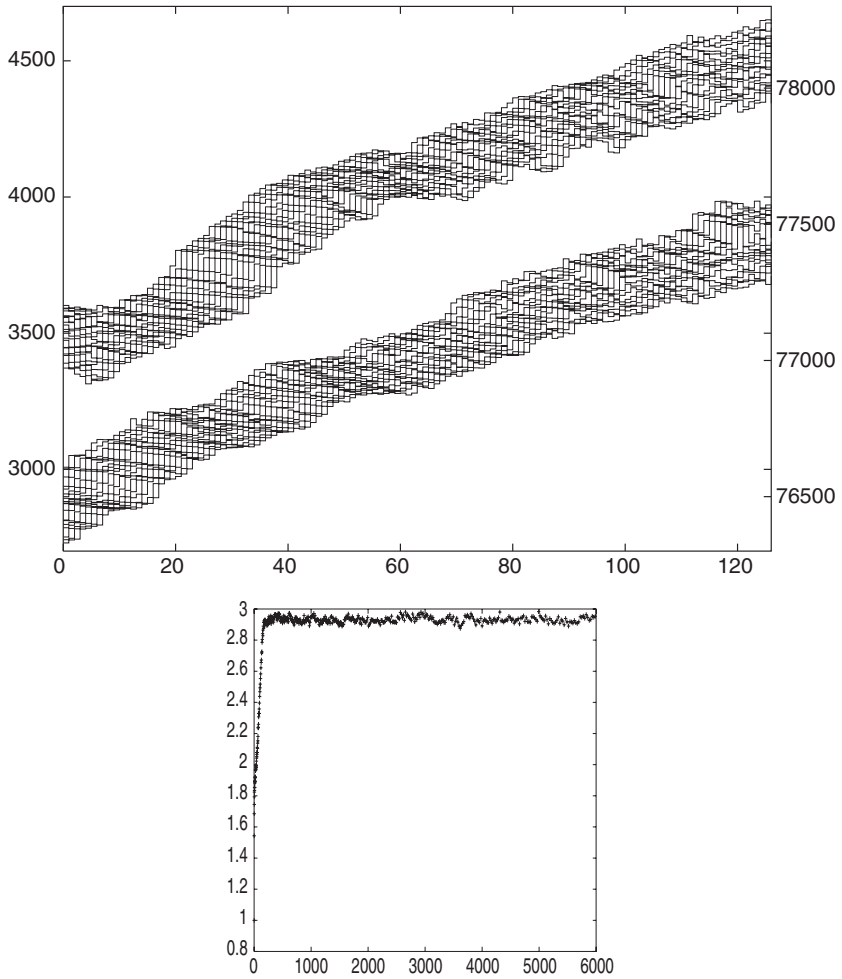

Figure 7. The gradient model (an inhomogeneous foam) of width $L = 250$. Top: layers around $j \sim 250$ (lower set, left vertical y scale) and around $j \sim 5000$ (upper set, right vertical y scale). The mean cell size is larger in the middle (on the right of the image) than on the left (the profile is symmetric wrt $x = L/2$, up to fluctuations). A steady state (slope, etc) has already been achieved in the lower set. Bottom: mean number of cells per layer and per column as a function of altitude (represented by the layer number j)(average over 50 samples).

6. Foams as clouds of defects

For concentric layers around a n-sided cell, it was observed that the number K_j of cells in layer j is the sum of two contributions [8]:

$$K_j = a(n-6) + b_j. \tag{8}$$

The second term, b_j, increases linearly with j (in 2D), as expected of smooth layers on a Euclidean, planar substrate. The first term does not depend on j. It is explained as follows: the central cell is the source of curvature, a topological charge $(n-6)$, which must be screened by the disordered foam. A dipole of opposite charge constitutes a dislocation, and screening of the 'central charge' is done by directing a few dipoles inevitably present in the random foam. Thus $a(n-6)$ is the Burgers vector resulting from the necessary screening of the topological

charge of the central cell by the random foam and K_j is proportional to the length of the closed contour encircling the central cell at distance j. The factor a is of the order of the screening length [26].

Our tower foam is also random, has non-hexagonal cells, and efficient screening by randomly oriented dislocations. Through periodic boundary conditions, each shell forms a closed contour, bounding a portion of the foam. This contour cuts across some dislocations, and its length fluctuates as the vector sum of the Burgers vectors of the dislocations which it cuts by an amount proportional to $L^{1/2}$. This argument is that of Kosterlitz and Thouless [27] to justify the existence of a condensed phase capable of resisting shear in two dimensions. The contour is called the Burgers contour or Wilson loop (more on this point in given in [26]).

7. Discussion

We have shown that the layer profiles have a shape similar to those observed in deposition–aggregation models and that scaling theory suitably accounts for their statistics. The layer number j is analogous to time in deposition processes.

The roughness of the layers obeys scaling power laws and the values of the exponents can be evaluated with good precision in our Cartesian model. The transverse fluctuations are controlled by a correlation length $\xi_j \propto j^{1/z}$ evolving in time (= distance to the origin) as a power law with exponent $z \simeq 1.5$. At horizontal length scales x small compared to ξ_j, the profile is rough. At larger length scales, the fluctuations are uncorrelated and the profile is reminiscent of the initial conditions. In the stationary regime, settled down in the range $x < \xi_j$, the roughness of the height (perpendicular to the layers) as a function of distance (parallel to the layers) obeys a power law $\delta h(x) \sim x^{\zeta}$. In our numerical simulations, we found $\zeta \simeq 0.5$. These values are in agreement with scaling and the KPZ universality class [19, 22, 23, 28].

Figure 3 shows clearly that the shape of the ground affects the statistics close to the bottom ($j = 0$), but this effect vanishes as we move away into the bulk. It is screened by the disorder. In fact, in cylindrical geometry, the saturation of the population K_j is much faster than the saturation of height fluctuations. This is due to the fact that shell length depends only on short range correlations which rapidly reach their stationary regime. The picture is similar to that of a random *directed* polymer, or to the fact that the macroscopic shape of aggregates is not fractal (even if their boundary is). Whence, in concentric geometry, M_j and K_j both have an asymptotic exponent $\nu = 1$ ($\nu = D - 1$ in higher dimensions) in the class of our models.

Immediately following from their definition, the fact that successive layers completely cover each other puts into the game a longitudinal nearest-neighbour correlation in a way which, apparently, has nothing to do with any specificity (correlation) of the (dis)order of the underlying cell pattern.

Similar conclusions can be drawn from the statistical distribution of dislocations; see [26].

In natural or simulated foams, shell j wiggles around, due to disorder, so that the perimeter of the topological circle of radius j is larger than $2\pi j$ or $6j$ (the value for a hexagonal honeycomb). The fact that K_j is linear in j (albeit with a slope larger than 6 as found in [9, 15] and here: see sections 3.6 and 5) shows that the disorder does not introduce some uniform, negative, Gaussian curvature[5]. The local fluctuations are controlled by the layer structure.

One last word about the model. One might object that our conclusions only hold for our special models, but we do not think so. The dominant phenomenon—saturation of the fluctuations—occurs in the vertical direction where the disorder is maximal (the height of our

[5] In a space of constant Gaussian curvature $-G$, a circle of radius j has perimeter equal to $\pi \left| G^{-1/2} \left[\exp(G^{1/2} j) - \exp(-G^{1/2} j) \right] \right|$.

cells are random and uncorrelated). Actually, the model was designed for this purpose: to shuffle, in a maximal way, the things in the direction where it is often implicitly believed, sometimes observed, that the layers only smoothly fluctuate.

Regarding other features, however, it is possible that maximal disorder has not quite been achieved in our model. One, obvious, bias is the strong anisotropy of our disorder, similar to the 'solid on solid' (SOS) approximation for solid surfaces: there is no backward or forward (in x) wandering of the layers (no overhangs in KPZs terminology [28]). Such wanderings would very probably change the topology of the layers (forming inclusions, for example).

Another artefact is the minimal size of the cells; even if there is always a natural UV cutoff in condensed matter, it may be irrelevant in the range of scales where the concept of foam applies (in this respect, our model is highly 'Euclidean'). Do these constraints affect the roughness of the layers? In principle, they could; in particular, when the (typical) cell sizes are not bounded from below, there is no more simple relation between the cell population K_j and the geometrical size M_j.

Nevertheless, we see no reason why the purely geometrical transverse rigidity of the layers, pointed out in the core of this paper, should not be present in any type of cell pattern. We conjecture that $\nu = 1$ holds generally in foams containing a bounded proportion of cells with vanishing size. In wilder cases without a lower bound in size, on the general argument that disorder increases roughness, our values of the exponents ζ and ν ought to be considered as lower bounds to real ones. Further investigations are on the way.

Acknowledgments

ChO thanks D Foster (LPTM, Cergy-Pontoise) for discussions, NR and the LDFC (Strasbourg) for hospitality.

Appendix. Defect inclusions

In general, the topology of the layers may be quite involved (see e.g. [16]). So, defining the basic concepts deserves some care, which is the purpose of this appendix.

First, notice that the boundary separating layer j from layer $j+1$ is not, in general, simply connected (in 2D, where none of the layers $j \geqslant 1$ are simply connected, we mean that this boundary may be topologically different from a circle). It is not even always connected, because the layers themselves may be disconnected; they may include 'baby universes', disjoint from the main layer (a concentric annulus in 2D).

So let us define a *shell* j as the *outer* boundary of layer j. In general, this is only a part of the boundary between layers j and $j+1$, namely the outermost connected part which has the topology of a $(D-1)$ sphere in dimension D. Its interior—the region of space containing the origin and bounded by shell j—contains all the cells of all the layers i with $i \leqslant j$. It may also contain cells from higher layers, 'baby universes', which are then also considered as inclusions.

The cells of layer j which share an edge (in 2D) or a face (in 3D) with shell j are called *regular* cells. The other ones are *defects*, or inclusions[6]. The defects of layer j either stick to regular j cells (on sides opposite to shell j, in such a way that the defects have no face in common with shell j), or they may form inclusion clusters, disconnected from the regular component (the part of the layer made of regular cells only). Such inclusions necessarily lie in the interior of some lower shell.

[6] This includes E and D defects of [8], 'type 2 and 3' cells of [10].

In figure 2, the defects are marked by a +. Proper inclusions (separated from the regular part) never occur in columnar models.

References

[1] Weaire D and Kermode J P 1983 *Phil. Mag.* B **47** L29
[2] Herdtle T and Aref H 1991 *Phil. Mag. Lett.* **64** 335
[3] Le Caer G and Delannay R 1995 *J. Physique* I (France) **5** 1417
[4] Aste T and Rivier N 1995 *J. Phys. A: Math. Gen.* **28** 1381–98
[5] Rivier N 1999 *Foams and Emulsions* ed J F Sadoc and N Rivier (Dordrecht: Kluwer) p 105
[6] Aste T, Boose D and Rivier N 1996 *Phys. Rev.* E **53** 6181
Rivier N and Aste T 1996 *Phil. Trans. R. Soc.* A **354** 2055
Aste T 1999 *Foams and Emulsions* ed J F Sadoc and N Rivier (Dordrecht: Kluwer) p 497
[7] Rivier N 1985 Jigsaw crystallography (unpublished notes)
Rivier N 1986 *Seminar* Imperial College
Troadec J P 1986 Echantillon construit grain par grain (unpublished notes)
[8] Dubertret B, Rivier N and Peshkin M A 1998 *J. Phys. A: Math. Gen.* **31** 879–900
[9] Ohlenbush H M, Aste T, Dubertret B and Rivier N 1998 *Eur. Phys. J.* B **2** 211–20
[10] Fortes M A and Pina P 1993 *Phil. Mag.* B **67** 263
[11] Binkmann G and Deza M 1998 *Liens* **98-13**
Binkmann G and Deza M 2000 *Hyperspace* **9** 28 (reprinted)
[12] O'Keeffe M 1995 *Z. Kristallogr.* **210** 905–8
O'Keeffe M and Hyde S T 1996 *Z. Kristallogr.* **211** 73–8
[13] Conway J H and Sloane J A 1997 *Proc. R. Soc.* A **453** 2369
[14] Baake M and Grimm U 1997 *Preprint* cond-mat/9706122
[15] Aste T, Szeto K Y and Tam W Y 1996 *Phys. Rev.* E **54** 5482–92
Szeto K Y, Aste T and Tam W Y 1998 *Phys. Rev.* E **58** 2656–9
[16] Magnasco M 1994 *Phil. Mag.* B **69** 397–429
[17] Stanley H E and Ostrowsky N (ed) 1986 *On Growth and Form (NATO ASI series E no 100)* (Dordrecht: Martinus Nijhoff)
[18] Godrèche C (ed) 1991 *Solids Far From Equilibrium* (Cambridge: Cambridge University Press)
[19] McKane A, Droz M, Vannimenus J and Wolf D (ed) 1995 *Scale Invariance, Interfaces, and Non-Equilibrium Dynamics (NATO ASI series B vol 344)* (New York: Plenum)
[20] See e.g. Delannay R and Le Caer G 1994 *Phys. Rev. Lett.* **73** 1553 and references therein
[21] Mombach J C, de Almeida R M and Iglesias J R 1993 *Phys. Rev.* E **47** 3712
[22] Sander L M 1991 *Solids Far From Equilibrium* ed C Godrèche (Cambridge: Cambridge University Press) pp 433-78
[23] Krug J and Spohn H 1991 *Solids Far From Equilibrium* ed C Godrèche (Cambridge: Cambridge University Press) pp 479–582
[24] Julien R and Botet R 1985 *J. Phys. A: Math. Gen.* **18** 2279
[25] Family F and Vicsek T 1985 *J. Phys. A: Math. Gen.* **18** L75
[26] Rivier N, Aste T, Dubertret B, Oguey C and Ohlenbusch H M 2001 Gauge invariance in foams, in preparation
[27] Kosterlitz J M and Thouless D J 1973 *J. Phys. C: Solid State Phys.* **6** 1181
[28] Kardar M, Parisi G and Zhang Y C 1986 *Phys. Rev. Lett.* **56** 889